JGR Space Physics

RESEARCH ARTICLE
10.1029/2019JA027293

A Statistical Study of Pi2 Pulsations Observed in the Upper Ionosphere Using Swarm Magnetic Field Data

Jae-Hee Park[1], Khan-Hyuk Kim[1], Hyuck-Jin Kwon[1], Geonhwa Jee[2,3], and Junga Hwang[4,5]

[1]School of Space Research, Kyung Hee University, Suwon, South Korea, [2]Division of Climate Change Research, Korea Polar Research Institute, Incheon, South Korea, [3]Department of Polar Science, University of Science and Technology, Daejeon, South Korea, [4]Korea Astronomy and Space Science Institute, Daejeon, South Korea, [5]Department of Astronomy and Space Science, University of Science and Technology, Daejeon, South Korea

Key Points:
- The ground satellite high coherence occurs when the spacecraft was located at $|\mathrm{MLAT}| \leq 50^{\circ}$
- The latitudinal structure of the relative amplitude and phase of the ionospheric Pi2 pulsations are examined
- The source of ionospheric Pi2 pulsations is the plasmaspheric resonance

Correspondence to:
K.-H. Kim.
khan@khu.ac.kr

Citation:
Park, J.-H., Kim, K.-H., Kwon, H.-J., Jee, G., & Hwang, J. (2020). A statistical study of Pi2 pulsations observed in the upper ionosphere using Swarm magnetic field data. *Journal of Geophysical Research: Space Physics*, *125*, e2019JA027293. https://doi.org/10.1029/2019JA027293

Received 13 AUG 2019
Accepted 9 NOV 2019
Accepted article online 23 NOV 2019

Abstract The properties of Pi2 pulsations observed in the upper ionosphere are studied using magnetic field data acquired by the Swarm A spacecraft in low Earth orbit and at the low-latitude Bohyun ground station (BOH, $L = 1.3$) for January 2014 to June 2015. From time intervals when Swarm A was on the nightside (magnetic local time (MLT) = 1800–0600 hr) and the BOH station was near midnight (MLT = 2100–0300 hr), we identified 621 Pi2 events in the horizontal H component of the BOH data. For each event we examined the coherence between the horizontal H component on the ground and the B_x (radial), B_y (azimuthal), or B_z (compressional) components at Swarm A. Out of 621 events, the B_x–H high-coherence (> 0.7) events are $\sim$ 6%, the B_y–H high-coherence events are $\sim$ 2%, and the B_z–H high-coherence events are $\sim$ 25%. The ground satellite high-coherence events occurred when the spacecraft was located at magnetic latitudes between −50° and 50°. Using the ground satellite high-coherence events, we statistically examined the latitudinal structure of the relative amplitude and phase of the ionospheric Pi2 pulsations and found that their latitudinal variations is consistent with the north-south mode structure expected from the plasmaspheric resonance model. Our statistical results indicate that the source of ionospheric Pi2 pulsations is the plasmaspheric resonance.

1. Introduction

Pi2 pulsations are damped oscillations of the geomagnetic field in the frequency range of $\sim$ 7–25 mHz (periods = $\sim$ 40–150 s). They are usually associated with the onset or intensification of magnetospheric substorms (Saito, 1969). Pi2 pulsations occur at all latitudes on the nightside (e.g., Olson, 1999) and are also observed at very low latitudes on the dayside (Shinohara et al., 1998; Sutcliffe & Yumoto, 1989). Although Pi2 pulsations have long been investigated, how and where they are established as a regular oscillation and what controls their frequency are not completely understood (e.g., Keiling & Takahashi, 2011).

At high latitudes (in the auroral zone) Pi2 pulsations are presumably transported to the ground by transient Alfven waves, which are associated with the field-aligned currents (FACs) (Bauer et al., 1995; Baumjohann & Glassmeier, 1984). High-latitude Pi2 pulsations are mainly observed in the region of substorm-enhanced ionospheric electrojet (e.g., Olson & Rostoker, 1975). Thus, their evolution is tied to the evolution of the substorm current system, and their period is determined by the Alfven travel time between the auroral ionosphere and the neutral sheet.

Pi2 pulsations observed on the ground at midlatitudes and low latitudes have a common frequency at different latitudes and over a wide range of longitudes. Such ground-based observations suggested that the cavity mode in the plasmasphere is a promising mechanism for low-latitude to midlatitude Pi2 pulsations (e.g., Lin et al., 1991; Stuart, 1974; Yeoman & Orr, 1989). Numerical studies showed that a well-defined cavity mode can be established in the plasmasphere by an impulsive disturbance associated with substorm onset (e.g., Fujita et al., 2002; Lee, 1996; Lee & Lysak, 1999; Takahashi et al., 2003; Takahashi, Hartinger, et al., 2018; Takahashi, Lysak, et al., 2018) or a driving source associated with fast mode pulses generated by the braking of periodic earthward bursty bulk flow (Lysak et al., 2015). If Pi2 oscillations are excited in the plasmasphere by the cavity resonance, their frequencies decrease as the plasmapause distance increases.

Combined Release and Radiation Effects Satellite (CRRES) observations inside the plasmasphere show the dependence of Pi2 frequency on the plasmapause distance (Takahashi et al., 2003). A statistical analysis of low-latitude Pi2 pulsations provides that the median period of Pi2 pulsations under quiet geomagnetic conditions ($Kp \leq 1$) is much longer ($\sim$ 214 s) than the conventional Pi2 period ($\sim$ 40–150 s) (Kwon et al., 2013). This may be due to the fact that the plasmapause is located at a large distance and thus the plasmaspheric resonance frequency becomes very low during periods of very low Kp. The plasmapaue is asymmetric along the local time with smaller (larger) plasmapause distance in the post(pre)midnight sector under moderate geomagnetic conditions (Kwon et al., 2015). It is expected that low-latitude Pi2 frequency is higher in the postmidnight sector than in the premidnight sector. Such local time-dependent Pi2 frequencies observed at low latitude and in the inner magnetosphere were reported by Kwon et al. (2012).

A ground satellite statistical study using magnetic field data simultaneously acquired by the Active Magnetospheric Particle Tracer Explorers Charge Composition Explorer (AMPTE CCE) and at low-latitude Kakioka ground station ($L =\sim 1.25$) reported that Pi2 pulsations in the nightside inner ($L = 2$–5) magnetosphere are fast-mode waves polarized in the meridian plane (Ohtani & Anderson, 1995). That is, the Pi2-associated magnetic field oscillations in the inner magnetosphere are dominated by the poloidal (δB_x and δB_z) components, and their phase and amplitude structures over a range of satellite radial distance ($L = 2$–5) and a dipole latitude range of $-16°$ to $16°$ support the cavity mode model. The authors found that ground satellite high-coherence events are observed primarily when the spacecraft is on the nightside and at $L < 4$. This indicates that low-latitude Pi2 pulsations observed on the ground originate from a cavity-mode-type resonance. Using the electric field and electron density data acquired on the CRRES in the inner magnetosphere, Takahashi et al. (2003) reported that the dusk-to-dawn (azimuthal) electric field component, representing the poloidal oscillation of the geomagnetic field lines, exhibited high coherence with low-latitude ground Pi2 when the satellite was located earthward of the plasmapause. The phase of the azimuthal electric field component relative to low-latitude horizontal northward (H) component is near $-90°$ over the radial distance of $L =\sim$ 2–6. These ground satellite observations provide evidence for the plasmaspheric origin of low-latitude Pi2 pulsations.

Pi2 pulsations have been identified in the upper ionosphere using low Earth orbit (LEO) magnetic field data. Takahashi and Yumoto (1999) examined a Pi2 event simultaneously observed by the Upper Atmosphere Research Satellite at an altitude of $\sim$ 580 km and at low-latitude stations in the Pacific. They reported that ionospheric magnetic field perturbation associated with the low-latitude Pi2 pulsation has radial and compressional components with waveform identical to the low-latitude Pi2 pulsation and that both the radial and compressional components at Upper Atmosphere Research Satellite oscillated in phase in the Northern Hemisphere. Sutcliffe and Lühr (2003) examined three Pi2 events using the magnetic field data obtained from CHAMP satellite in LEO and at a low-latitude station. The radial and compressional components at CHAMP are highly correlated with the H component of the Pi2 pulsations at the low-latitude ground station. The radial and compressional oscillations are in phase in the Northern Hemisphere and out of phase in the Southern Hemisphere. This is consistent with AMPTE CCE observations at $L = 2$–4 (Ohtani & Anderson, 1995). Han et al. (2003) statistically analyzed Pi2 pulsations observed by Ørsted satellite in LEO and at a low-latitude station. They found that the compressional oscillations at Ørsted are highly correlated with the low-latitude H component Pi2 oscillations, but the radial oscillations have a low correlation with the ground Pi2 events. These previous studies of Pi2 pulsations using LEO magnetic field data in the upper ionosphere suggested that ionospheric Pi2 pulsations are associated with the plasmaspheric resonance mode. Most recently, Thomas et al. (2019) examined 15 high-coherence compressional Pi2 events simultaneously detected by the Swarm spacecraft in the upper ionosphere and at low-latitude ground station. They suggested that the source for nighttime Pi2 pulsations observed in the ionosphere and at low-latitude are oscillating FACs. Kim et al. (2019) examined four Pi2 events identified from low-latitude ground station near midnight while Swarm spacecraft were orbiting in the premidnight meridian. Unlike Thomas's suggestion not requiring plasmaspheric resonances, Kim et al. (2019) reported that the latitudinal phase and amplitude relationships between the radial and compressional magnetic field oscillations at Swarm are the consequence of the spatial mode structure in the north-south direction of trapped fast mode waves inside the plasmasphere.

In this paper we extend the case Swarm study by Kim et al. (2019) to statistically examine whether the amplitude and phase variations of the ionospheric Pi2 pulsations is consistent with the latitudinal structure expected from the plasmaspheric resonance model. Unlike previous ionospheric Pi2 studies, we investigate the spectral intensity, coherence, and phase of the ionospheric magnetic field perturbations in the radial B_x,

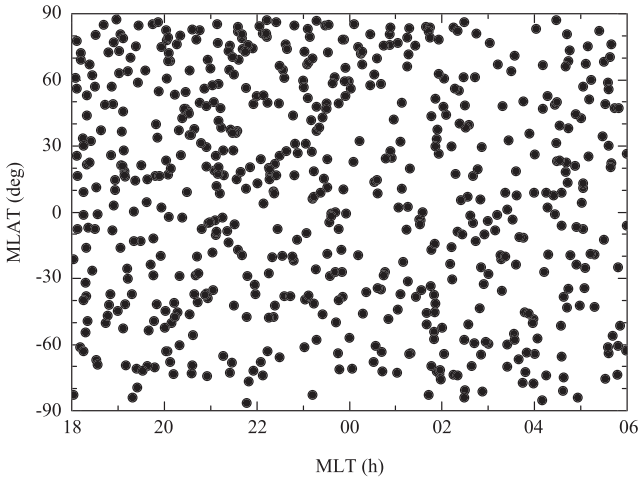

Figure 1. Location of Swarm A at the time of a Pi2 pulsation observed at low-latitude Bohyun station in South Korea.

azimuthal B_y, and compressional B_z components observed at the LEO Swarm A spacecraft relative to those of low-latitude Pi2 pulsations in the horizontal H component. We show that ground satellite high-coherence events occurred when the spacecraft was located within a magnetic latitude range of ±50°. We also show that the relative amplitude and cross phase between the radial and compressional components strongly depend on the latitude of the satellite and that the latitudinal variations are consistent with previous results of magnetospheric Pi2 pulsations observed in the inner magnetosphere.

The organization of the paper is as follows. In Section 2 we describe the data set and event selection. In Section 3 we examine one ionospheric Pi2 event. In Section 4 we describe the results of the statistical analysis of the high-coherence events. In Section 5 we discuss possible source mechanisms for ionospheric Pi2 pulsations. Section 6 presents the conclusions.

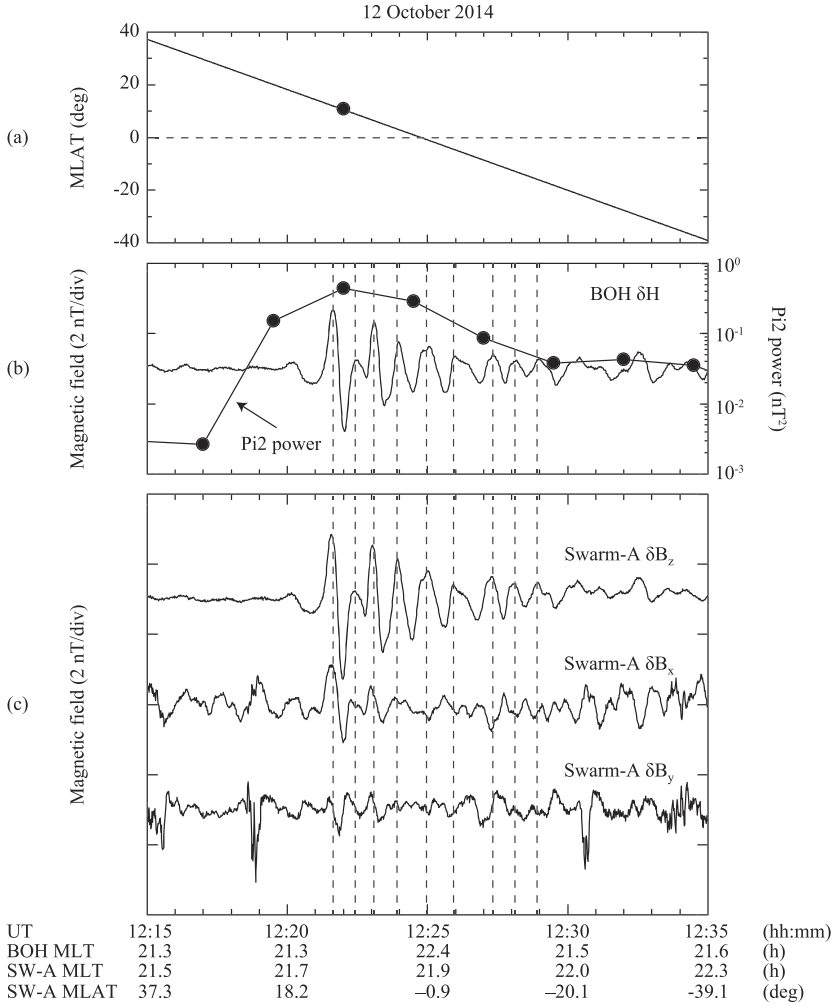

Figure 2. (a) The magnetic latitude of Swarm A, (b) time series of Bohyun δH and Pi2 power, and (c) Swarm A δB_z, δB_x, and δB_y for the interval from 12:15 to 12:35 UT on 12 October 2014. The solid dot in (a) indicates the Swarm A location in MLAT at the time of the maximum power of Pi2 pulsation.

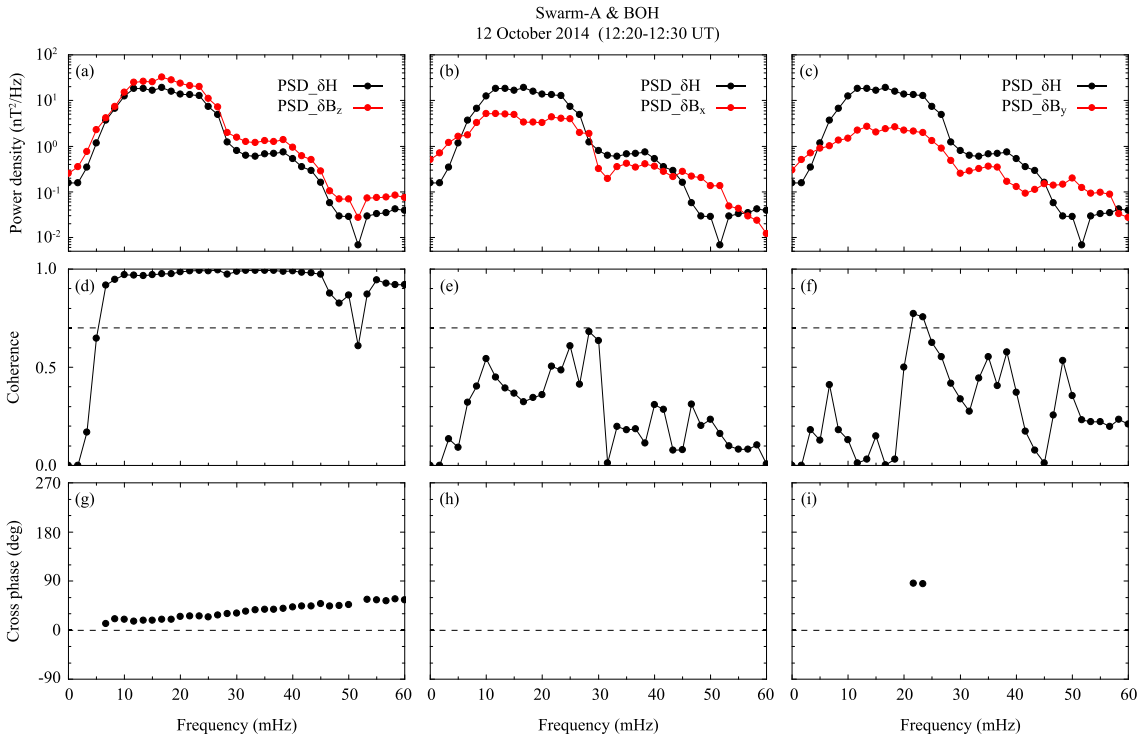

Figure 3. Ground satellite spectral analysis of the Pi2 pulsation shown in Figure 2. The spectral density, coherence, and cross phase of the three components (δB_z, δB_x, and δB_y) at Swarm A are calculated using as a reference signal of the Bohyun δH.

2. Data

2.1. Data Set

We use magnetic field data measured in the ionosphere by the Swarm Alpha (Swarm A) spacecraft, which is one of the Swarm constellation consisting of three satellites (Swarm A, Swarm Charlie [Swarm C], and Swarm Bravo [Swarm B]), and at the low-latitude Bohyun ground station from January 2014 to June 2015. The three Swarm spacecraft were launched on 22 November 2013 and placed in two different polar orbits: Swarm A and Swarm C have been flying side by side on a nearly identical orbit at ∼ 460 km altitude with latitudinal and longitudinal separations less than 1.5° and an inclination of 87.4°, and Swarm B has been operated at a slightly higher altitude of ∼ 510 km with an inclination of 87.8° (Friis-Christensen et al., 2008; Olsen et al., 2013). The Swarm B and Swarm C data were available for this study, but we do not use the data because their orbits were very similar to the Swarm A orbits, making some observations redundant.

Swarm A magnetic field data used in the present study are 1-s samples acquired with the vector fluxgate magnetometer. The original vector fluxgate magnetometer data were provided in the North-East-Center local Cartesian coordinate frame in which $\hat{\mathbf{N}}$ is the direction of geographic north, $\hat{\mathbf{E}}$ points geographic east, and $\hat{\mathbf{C}}$ points toward the center of the Earth. In order to enhance ionospheric Pi2 pulsations, the crustal magnetic field is removed from the observed ionospheric magnetic field data using the CHAOS-5 model (Finlay et al., 2015), and then a second-order polynomial fitted to the original data for each component in North-East-Center coordinates is also removed. To separate the ionospheric magnetic field perturbations into the toroidal and poloidal components, the Swarm magnetic field data are rotated into magnetic field-aligned coordinates using the measured local magnetic field as the reference. In this system, the compressional (or parallel) component $\hat{\mathbf{e}}_z$ is along the measured magnetic field direction; the azimuthal component $\hat{\mathbf{e}}_y$ (positive eastward) is in the direction of $\hat{\mathbf{e}}_z \times \mathbf{r}$, where $\mathbf{r}$ is the radial vector pointing from the center of the Earth toward the spacecraft; and the radial component $\hat{\mathbf{e}}_x$ (positive outward) is given by $\hat{\mathbf{e}}_x = \hat{\mathbf{e}}_y \times \hat{\mathbf{e}}_z$.

Previous numerical studies (e.g., Lin et al., 1991; Allan et al., 1996) reported that the radial and compressional components of a fastmode wave in the magnetosphere directly map to the H component of the low-latitude Pi2 pulsation on the ground. In this study, the low-latitude Pi2 pulsation in the horizontal

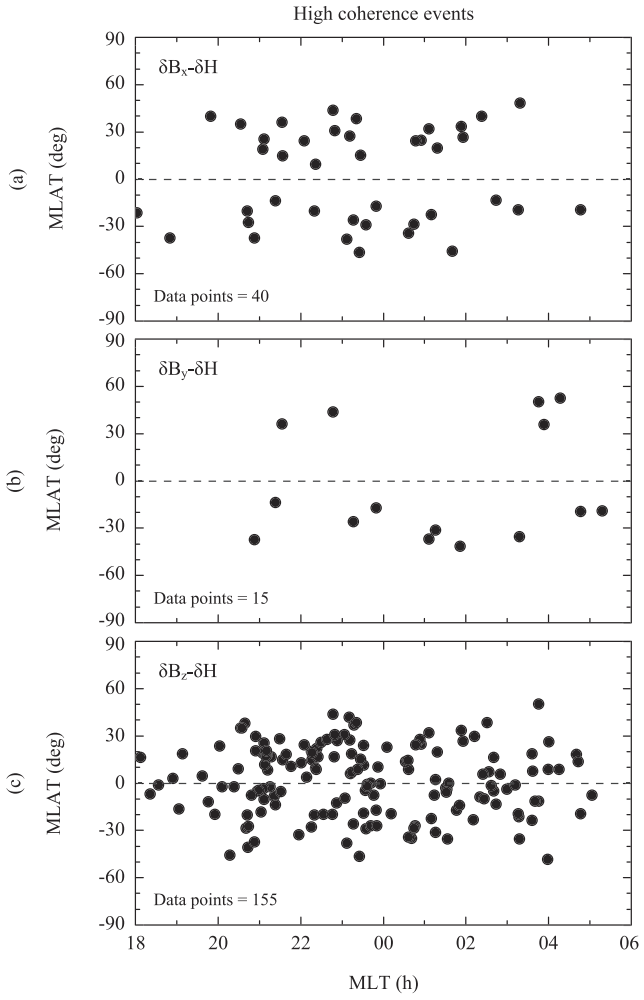

Figure 4. The occurrence distribution of ground satellite high-coherence events for (a) $\delta B_x - \delta H$, (b) $\delta B_y - \delta H$, and (c) $\delta B_z - \delta H$ in the MLAT-MLT plot.

H (positive northward) component is used as a reference signal for a study of ionospheric Pi2 pulsation. We use magnetometer data from the low-latitude Bohyun (BOH) station in South Korea to identify low-latitude Pi2 pulsations. BOH is located at a magnetic latitude (MLAT) of 29.8° ($L = \sim 1.3$, local time ~ UT+9 hr), a geographic latitude of 36.2°, and a geographic longitude of 128.9°. BOH provides fluxgate magnetometer data with 1-s sampling.

2.2. Low-Latitude Pi2 Event Selection

We used the semiautomated procedure developed by Kwon et al. (2013) to identify low-latitude Pi2 pulsations from the H component of the BOH magnetic field data when the BOH station was near midnight between 2100 and 0300 magnetic local time (MLT). In the semiautomated procedure, the Pi2 event is selected in Pi2 power time series, which is defined as the integral of the power spectral density over the fixed Pi2 (6.6- to 25-mHz) band. The Pi2 power is calculated from the 10-min BOH H data filtered by removing 180-s running averages, with 25% overlap of successive Fourier transform data windows. We impose the power threshold of 0.02 $(\text{nT})^2$ in event selection to ensure sufficient wave power and identified 621 low-latitude Pi2 events for the interval from January 2014 to June 2015. While the Pi2 events were identified at BOH, Swarm A was in the nightside from 18 to 06 MLT. Figure 1 shows Swarm A locations at times of the power maximum of Pi2 pulsations detected at BOH in the MLAT-MLT plot.

3. Example of Ionospheric Pi2 Pulsation

Figure 2 shows the time series plots of δH at BOH and δB_x, δB_y, and δB_z at Swarm A with the position of the satellite in MLAT and BOH Pi2 power for the interval of 12:15–12:35 UT on 12 October 2014. The solid dot in Figure 2a indicates the Swarm A location in MLAT at time of the maximum power of Pi2 pulsation. The low-latitude Pi2 pulsation starting at ~ 12:21 UT was observed while Swarm A was crossing the magnetic equator from the Northern Hemisphere to the Southern Hemisphere. During the Pi2 event, Swarm A and BOH were in the premidnight sector (MLT = ~ 21 hr) with a small local time separation less than 0.5 hr. The vertical dashed lines indicate the peaks of δH. The magnetic field perturbations in δB_z at Swarm A and δH at BOH are seen with nearly identical waveforms without significant phase delay, and their amplitudes are comparable. The high similarity of the waveforms between the ionosphere and ground suggests that the pulsations are excited by a common source mechanism. At Swarm A δB_z and δB_x oscillate exactly in phase for the first four cycles when the satellite was above the equator, but their amplitudes are not equal: δB_z is larger than δB_x by a factor of ~ 2. At the equator, there is no perturbation in δB_x, and then antiphase oscillations between δB_z and δB_x appeared for the last three cycles when the satellite was below the equator. There are oscillations in δB_y, but their waveforms and period do not match δH. This indicates that the δB_y oscillation does not have a direct relation with the δH oscillations.

The similarity in waveforms between the ionosphere and the ground can be confirmed by ground satellite coherence analysis in the frequency domain. Figure 3 compares the spectral properties of δH at BOH and the three field components (δB_x, δB_y, and δB_z) at Swarm A for the interval of 12:20–12:30 UT. The spectral parameters were obtained by Fourier transforming the time series and then by taking the average over five spectral estimates. The cross phase is shown only for the frequencies at which the coherence is higher than 0.7. As expected from the waveform plots of Figure 2b, the power spectra for δH and δB_z show a dominant spectral enhancement centered at around 17 mHz with a nearly identical spectral shape. The $\delta B_z - \delta H$ coherence at the spectral enhancement is near perfect, and the cross phase is close to 0°. The δB_x spectral power also shows an enhancement centered at ~ 17 mHz, but the $\delta B_x - \delta H$ coherence calculated for the

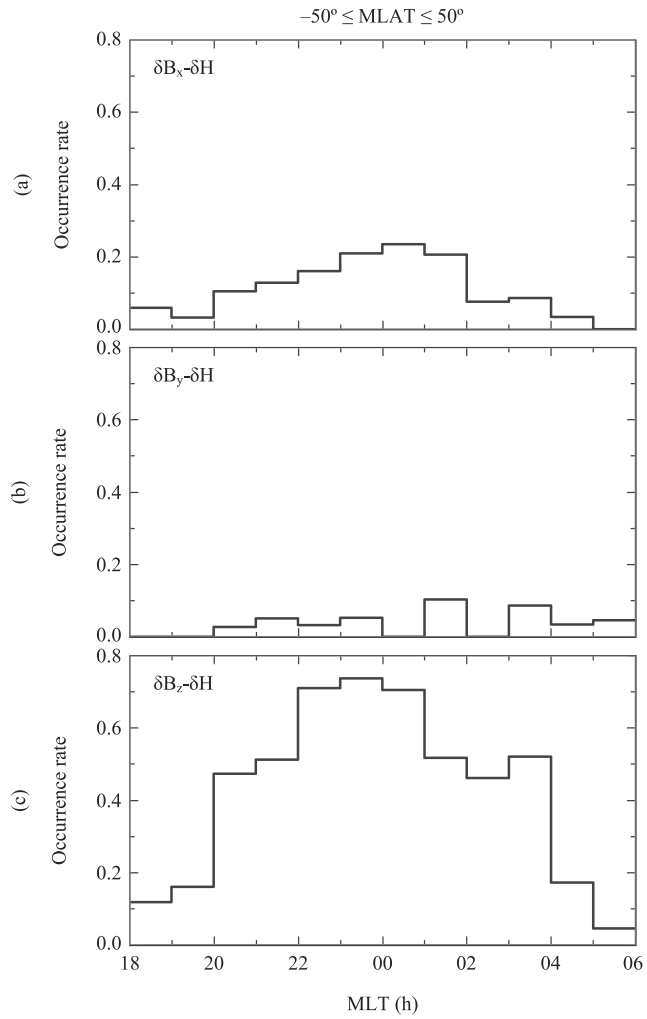

Figure 5. The occurrence rate of the ground satellite high-coherence events in the −50° ≤ MLAT ≤ 50° region. (a) $\delta B_x - \delta H$, (b) $\delta B_y - \delta H$, and (c) $\delta B_z - \delta H$.

10-min interval is lower than 0.7 at the spectral enhancement. This low coherence is due to the fact that the phase delay and amplitude ratio between δB_x and δH are not constant for a time interval of low-latitude Pi2 pulsation. The power spectrum of δB_y produces a broad peak near 17 mHz, and the δB_y power is smaller than the δH power by a factor of 10. The $\delta B_y - \delta H$ coherence shows spectral estimates higher than 0.7 at $\sim$ 22–23 mHz but rapidly decreases to a value less than 0.2 at frequencies of $\sim$ 10–18 mHz in the spectral enhancement of δH. Since the δB_y oscillations did not last for the interval of low-latitude Pi2 pulsation, we do not consider he δB_y oscillations with the $\delta B_y - \delta H$ high-coherence spectral estimates as a ground satellite high-coherence event.

4. Statistical Analysis

In this section we present a statistical analysis of ground satellite high-coherence events (coherence between Swarm A and BOH > 0.7). Out of 621 low-latitude Pi2 events identified at BOH, 155 ($\sim$ 25%) events exhibited high $\delta B_z - \delta H$ coherence, 40 ($\sim$ 6%) exhibited high $\delta B_x - \delta H$ coherence, and 15 ($\sim$ 2%) exhibited high $\delta B_y - \delta H$ coherence. This statistical result indicates that most of low-latitude Pi2 events do not have a direct relation with the δB_y oscillations at Swarm A. Figure 4 shows the occurrence distribution of ground satellite high-coherence events in the MLAT-MLT plot. The high-coherence events occurred when the spacecraft was located within a magnetic latitude range of ±50°. There are no high $\delta B_x - \delta H$ and $\delta B_y - \delta H$ coherence events near the equator.

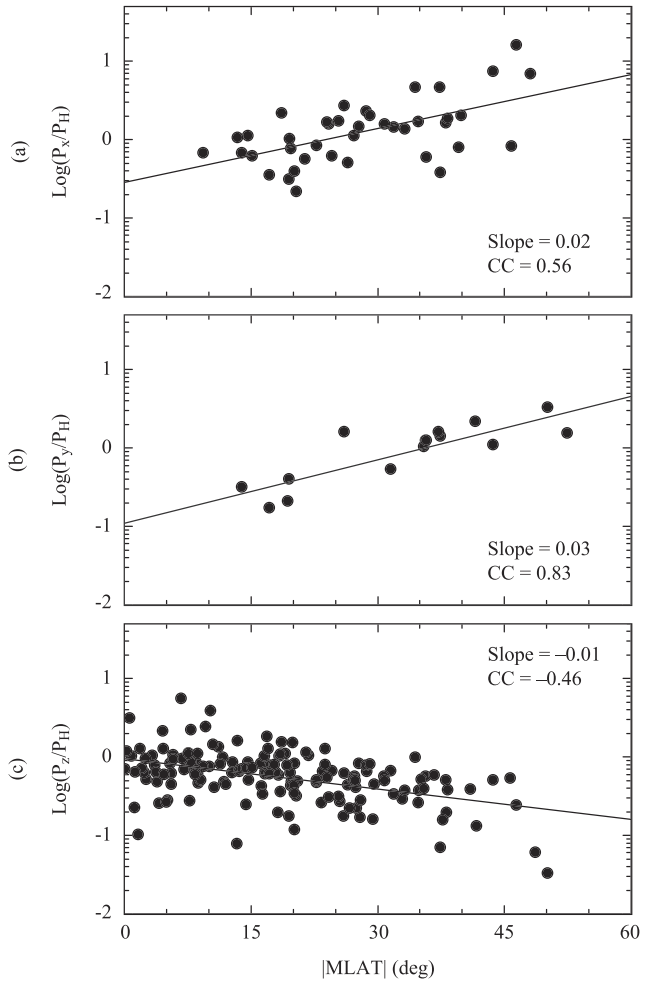

Figure 6. The latitudinal amplitude variation of the power ratios (a) $\delta B_x/\delta H$, (b) $\delta B_y/\delta H$, and (c) $\delta B_z/\delta H$ for high-coherence events. The slope of the fitted line and the linear correlation coefficient (CC) between the latitude and the power ratio are given in each plot.

Figure 5 shows the occurrence rate of the ground satellite high-coherence events in the $-50° \leq$ MLAT $\leq 50°$ region. The occurrence rate was obtained by dividing the number of high-coherence events by the total number of events in the MLAT range of $-50°$ to $50°$ for each 1-hr MLT bin. The occurrence rate of δB_z–δH high-coherence events (Figure 5) is strongly peaked in the 2200–0100 MLT sector. About 72% (62 out of 86 events) of δB_z oscillations at Swarm A in this local time sector have high coherence with low-latitude Pi2 events at BOH. This local time dependence, which is slightly asymmetric with respect to midnight, may be due to a similarly asymmetric distribution of Pi2 energy source (Takahashi & Liou, 2004). In the 2000–2200 MLT and 0100–0400 MLT sectors, the occurrence rate of δB_z–δH high-coherence events is above 40%. This indicates that well-defined Pi2-associated δB_z oscillations are distributed in the nightside ionosphere. The occurrence rate of the δB_x–δH high-coherence events is about 10–20% within 4 hr of midnight. The occurrence rate of the δB_y–δH high-coherence events is less than 10% in the 1800–0600 MLT sector without a peak near midnight.

In order to examine the latitudinal amplitude variation of high-coherence events, the power of δB_x (P_x), δB_y (P_y), and δB_z (P_z) normalized to the power of δH (P_H) as a function of the absolute magnetic latitude (|MLAT|) of Swarm A are plotted in Figure 6 with the slope determined by least squares fitting and the linear correlation coefficient. As shown in Figure 4, there are no δB_x–δH and δB_y–δH high-coherence events near the equator. The δB_x and δB_y oscillations having high coherence with low-latitude Pi2 events were observed when Swarm A was away from the equator (|MLAT| > 15°). The normalized δB_x and δB_y powers in logarithmic scale exhibit a clear increasing function of |MLAT|. A linear regression analysis yields a

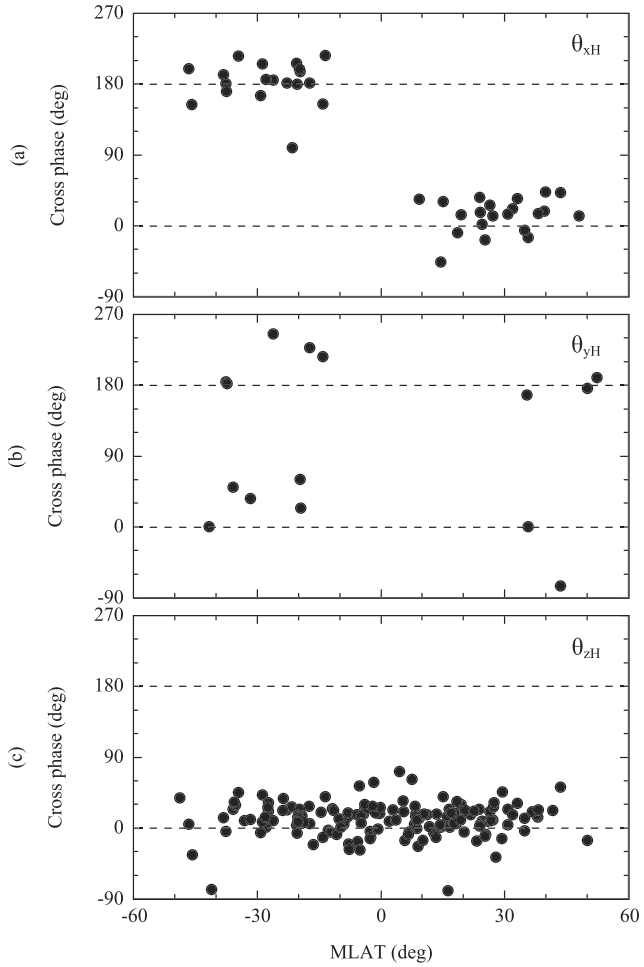

Figure 7. The (a) $\delta B_x - \delta H$, (b) $\delta B_y - \delta H$, and (c) $\delta B_z - \delta H$ cross phase for high-coherence events as a function of MLAT.

correlation coefficient of 0.56 for P_x/P_H and 0.83 for P_y/P_H, respectively. The normalized compressional δB_z power shows an opposite trend. That is, P_z/P_H decreases as |MLAT| increases. The correlation coefficient is −0.46. These latitudinal variations of the normalized power of δB_x, δB_y, and δB_z oscillations observed in the ionosphere are similar to those of Pi2 waves observed in the nightside inner magnetosphere ($L < 4$) (Ohtani & Anderson, 1995) and Pc3 waves observed in the dayside inner magnetosphere($L < 3$) (Kim & Takahashi, 1999), having a north-south standing mode structure: δB_x and δB_y have a node, and δB_z has an antinode at the magnetic equator because of a symmetric field line displacement about the equator.

Figure 7 shows the $\delta B_x - \delta H$, $\delta B_y - \delta H$, and $\delta B_z - \delta H$ cross phase for high-coherence events as a function of MLAT. The $\delta B_x - \delta H$ cross phase is distributed near 0° in the Northern Hemisphere and 180° in the Southern Hemisphere. However, the data points of the $\delta B_z - \delta H$ cross phase are clustered at ~ 0° without a clear latitudinal dependence. The $\delta B_x - \delta H$ and $\delta B_z - \delta H$ cross phases are also similar to those obtained for Pi2 pulsations observed in the nightside inner magnetosphere (Ohtani & Anderson, 1995) and Pc3 pulsations observed in the dayside inner magnetosphere (Kim & Takahashi, 1999) by the CCE satellite at geomagnetic latitudes from −16° to 16°. The previous CCE observations have been taken as evidence of a cavity mode oscillation in the inner magnetosphere. The latitudinal phase structure of $\delta B_y - \delta H$ is significantly different from that of $\delta B_x - \delta H$ and $\delta B_z - \delta H$. There are two groups for the $\delta B_y - \delta H$ cross phase in the Southern Hemisphere. One is distributed in the 0° to 90° range, and the other is in the 180° to 270°. In the Northern Hemisphere, there are five data points. Three of them are distributed near 180°, and two of them are 0° and −90°.

Figure 8 shows the local time dependence of the $\delta B_x - \delta H$, $\delta B_y - \delta H$, and $\delta B_z - \delta H$ cross phase. Most of the data points of the $\delta B_x - \delta H$ phase are distributed in a range of ~ 150–240° centered at about 180° in the Southern Hemisphere and of ~–60° to 60° centered at about 0° in the Northern Hemisphere. They do not show a clear

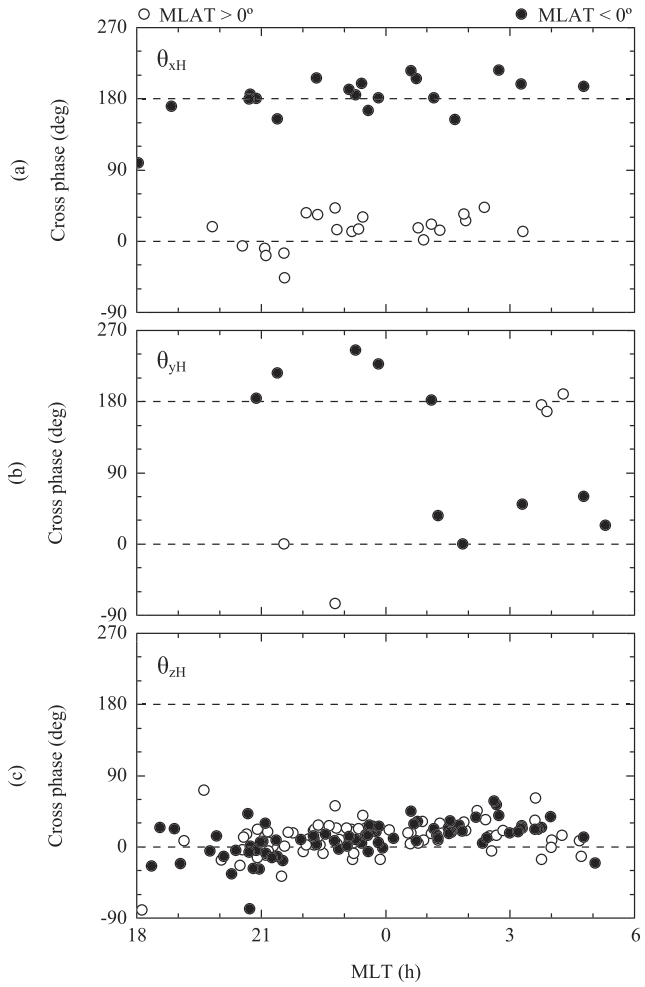

Figure 8. The local time dependence of the (a) $\delta B_x - \delta H$, (b) $\delta B_y - \delta H$, and (c) $\delta B_z - \delta H$ cross phase. The solid (open) circles indicate observations in the Southern (Northern) Hemisphere.

local time dependence. The data points of the $\delta B_z - \delta H$ phase in Figure 8c are scattered around 0° without a dependence on the latitude of the satellite relative to the magnetic equator. Unlike $\delta B_x - \delta H$ and $\delta B_z - \delta H$ phases, the $\delta B_y - \delta H$ phase shows a clear local time dependence. When the satellite was in the Southern Hemisphere, the data points of the $\delta B_y - \delta H$ phase are distributed in the 180° to 270° region in the premidnight sector and in the 0° to 90° region in the postmidnight sector. Although there are small data points in the Northern Hemisphere, they show an opposite trend. That is, the $\delta B_y - \delta H$ phase is in the −90° to 0° region in the premidnight sector and ∼ 180° in the postmidnight sector.

5. Discussion

It has been reported that Pi2 pulsations observed in the inner magnetosphere are generated by plasmaspheric cavity mode resonances. If a cavity mode is excited in the plasmasphere, the transverse radial δB_x and compressional δB_z components should exhibit a standing wave structure in the radial and north-south directions in the meridional plane of the plasmasphere. A simulation study of fundamental plasmaspheric cavity mode shows that the radial mode structure of δB_z has a node at a point very close to the plasmapause and that δB_z gives a 180° phase shift across the nodal point along the radial direction (Lee & Lysak, 1999; Takahashi et al., 2003). Many satellite observations in the inner magnetosphere provide evidence in support of plasmaspheric cavity mode as the source of low-latitude Pi2 pulsations. (Ohtani & Anderson, 1995) reported that the coherence between Pi2 pulsations observed in the H component at the low-latitude Kakioka station ($L =\sim 1.25$) and magnetic field perturbations detected by the AMPTE CCE spacecraft is

high when the spacecraft is on the nightside and at $L < 4$. In that region, Pi2-associated magnetic field pulsations are excited primarily in the δB_x and δB_z components. The authors indicated that the radial variations of the amplitude and phase of δB_x and δB_z oscillations are consistent with the eigenmode structure of a compressional cavity-mode-type resonances excited between two reflecting boundaries. The Pi2-associated electric and magnetic field oscillations observed from CRRES (Takahashi et al., 2003), THEMIS probes (Kim et al., 2010; Kwon et al., 2012), and Van Allen Probes (Ghamry et al., 2015) in the inner magnetosphere provide a clear evidence for a radially standing fastmode signature. These spacecraft observations show that the low-latitude Pi2 pulsations are related to fastmode waves trapped inside the plasmasphere.

A standing structure in the north-south direction is also expected when an ideal cavity mode is excited in the plasmasphere. Previous observations suggest that Pi2 pulsations observed in the nightside inner magnetosphere (Ohtani & Anderson, 1995) and Pc3 pulsations observed in the dayside magnetosphere (Kim & Takahashi, 1999) have a symmetric field line displacement pattern about the magnetic equator. This means that δB_x (δB_z) has a node (an antinode) at the magnetic equator, and thus the power of δB_x (δB_z) increases (decreases) with latitude. Such latitudinal amplitude variations of δB_x and δB_z have been confirmed in the numerical study of plasmaspheric resonances (Lee, 1996; Teramoto et al., 2011). For the north-south standing mode structures of δB_x and δB_z, the cross phase between δB_x and δB_z depends on the location about the magnetic equator. That is, the cross phase is 0° in the Northern Hemisphere and 180° in the Southern Hemisphere inside the nodal point of δB_z along the radial direction (e.g., Sutcliffe & Lühr, 2003). Using the magnetic field data obtained from CCE spacecraft covering a dipole magnetic latitude rage from −16° to +16°, Takahashi et al. (1995) statistically examined the latitudinal amplitude and cross phase variations of Pi2-associated magnetic field variations in δB_x and δB_z. In their study, they showed that the latitudinal structure of δB_x and δB_z observed in a radial distance of $L = 2$–4 is consistent with the north-south standing mode structure of δB_x and δB_z in an ideal cavity model.

In order to examine whether the north-south mode structure of cavity-type magnetospheric Pi2 pulsations reported by the AMPTE CCE study at $L > 2$ and at |MLAT| ≤ 16° extends down to the upper ionosphere ($L < 2$), we have studied the statistical properties of ionospheric Pi2 pulsations using magnetic field data simultaneously acquired by the Swarm A spacecraft, covering all MLAT, in the nightside (MLT = 18–06 hr) upper ionosphere and at the low-latitude BOH station ($L =\sim 1.3$) near midnight (MLT = 21–03 hr) for ground satellite high-coherence events. We found that the δB_z−δH high-coherence events are ∼ 25% (155 out of 621 events) of the low-latitude BOH Pi2 events. These high-coherent events are observed when Swarm A is located at |MLAT| ≤ 50°. It should be noted that there are coherent δB_z oscillations in the region of |MLAT| > 50°. However, the coherent signature of δB_z oscillations did not last for the low-latitude Pi2 interval (∼ 10 min) because the spacecraft enters the auroral region in which there are strong non-Pi2 signals masking Pi2 waves and destroying coherence. There are δB_x and δB_y oscillations highly coherent with low-latitude Pi2 waves. However, only ∼ 6% δB_x and ∼ 2% δB_y oscillations are associated with low-latitude Pi2 waves.

For the high-coherence events we examined the latitudinal amplitude variation. We found that the δB_z power is a decreasing function of latitude, whereas δB_x and δB_y powers are increasing functions. The latitudinal structures of δB_z and δB_x wave powers are consistent with the north-south eigenmode structure of cavity-type plasmaspheric resonances. The cross phases between δB_z and δH are distributed near 0° without depending on the latitude of the satellite, whereas the δB_x−δH cross phases are near 0° in the Northern Hemisphere and about 180° in the Southern Hemisphere. Since the low-latitude Pi2 wave is used as a reference signal, the latitudinal phase structures of δB_x−δH and δB_z−δH imply that the δB_x−δB_z cross phase is 0° in the Northern Hemisphere and 180° in the Southern Hemisphere. These latitudinal phase variations can be taken as evidence for the north-south mode structure of a plasmaspheric resonances. In Figure 6, we found the absence of the high-coherence δB_x−δH events near the equator. It should be noted that the relative phase and amplitude of δB_x and δH need to be constant for high coherence (Takahashi et al., 2001). As the LEO satellite is approaching and crossing the equator, the power and phase of δB_x change relatively to δH. Such relative phase and amplitude changes destroy coherence. According to numerical studies of plasmaspheric resonances (Lysak et al., 2015; Teramoto et al., 2011), the compressional wave trapped in the plasmasphere is confined in a dipole latitude rage of −40° < MLAT < 40°. The Swarm A spacecraft's orbital speed is ∼3.8°/min, and thus the spacecraft covers ∼38° MLAT in a 10-min interval, indicating that the 10-min segments of the Swarm A data obtained near the equator include the equatorial crossing. This is the reason why we have the small number of the high-coherence δB_x−δH events.

Recently, Thomas et al. (2019) have proposed that Pi2 oscillations observed in the nightside low to middle latitude ionosphere are associated with FACs flowing on substorm current wedge and mapping to the auroral zone ionosphere. If the ionospheric Pi2 pulsations originate from oscillating FACs, the negative (positive) δB_y perturbation is expected in a region located east (west) of the center of substorm current wedge in the Northern Hemisphere due to a downward (upward) FAC and vice versa in the Southern Hemisphere (see Figure 9 in Thomas et al., 2019). Consequently, the cross phase between δB_y and δH is 0° in the premidnight sector and 180° in the postmidnight sector in the Northern Hemisphere and 180° in the premidnight sector and 0° in the postmidnight sector in the Southern Hemisphere. We observed that the $\delta B_y - \delta H$ high-coherence events are $\sim$ 2%. The local time variation of their cross phases shown in Figure 8 is similar to the phase change of δB_y expected from the FACs model. Thus, all high-coherence events in our study do not fit the cavity-type model.

6. Conclusions

We have studied the properties of Pi2 pulsations observed simultaneously by the Swarm A spacecraft in the nightside ionosphere and at low-latitude Bohyun station ($L = 1.3$). High coherence between the horizontal H component on the ground and the B_x (radial), B_y (azimuthal), or B_z (compressional) components at Swarm A are examined. We found that the $\delta B_z - \delta H$ high-coherence events are ~25%, $\delta B_x - \delta H$ high-coherence events are $\sim$ 6%, and $\delta B_y - \delta H$ high-coherence events are $\sim$ 2%. The high-coherence events were observed when the Swarm A was in $|\text{MLAT}| \leq 50°$. The latitudinal variations of the relative amplitude and phase of the ionospheric δB_x abd δB_z oscillations are consistent with previous results of magnetospheric Pi2 pulsations observed in the inner magnetosphere, which are favoring a cavity mode-type oscillation. This indicates that cavity-type magnetospheric Pi2 pulsations extend down to the upper ionosphere.

Acknowledgments
Swarm data used in this study are available online (at https://earth.esa.int/web/guest/swarm/data-access). The Bohyun magnetic field data were provided by the Solar and Space Weather Research Group in Korea Astronomy and Space Science Institute (KASI). This work was supported by BK21+ through the National Research Foundation (NRF) funded by the Ministry of Education of Korea. The work of K.-H. Kim was supported by the Basic Science Research Program through NRF funded by NRF-2019R1F1A1055444 and also supported by Project PE19020 of the Korea Polar Research Institute. The work of J. Hwang was supported by the basic research funding from KASI.

References

Allan, W., Menk, F. W., Fraser, B. J., Li, Y., & White S. P. (1996). Are low-latitude Pi2 pulsations cavity/waveguide modes? *Geophysical Research Letters*, *23*(7), 765–768. https://doi.org/10.1029/96gl00661

Bauer, T. M., Baumjohann, W., & Treumann, R. A. (1995). Neutral sheet oscillations at substorm onset. *Journal of Geophysical Research*, *23*, 737.

Baumjohann, W., & Glassmeier, K.-H. (1984). The transient response mechanism and Pi2 pulsations at substorm onset: Review and outlook. *Planetary and Space Science*, *32*, 1361.

Finlay, C. C., Olsen, N., & Toeffner-Clausen, L. (2015). DTU candidate field models for IGRF-12 and the CHAOS-5 geomagnetic field model. *Earth Planets Space*, *67*, 114. https://doi.org/10.1186/s40623-015-0274-3

Friis-Christensen, E., Lühr, H., Knudsen, D., & Haagmans, R. (2008). Swarm. An Earth observation mission investigating geospace. *Advances in Space Research*, *41*(1), 210–216. https://doi.org/10.1016/j.asr.2006.10.008

Fujita, S., Nakata, H., Itonaga, M., Yoshikawa, A., & Mizuta, T. (2002). A numerical simulation of the Pi2 pulsations associated with the substorm current wedge. *Journal of Geophysical Research*, *107*(A3), 1034. https://doi.org/10.1029/2001JA900137

Ghamry, E., Kim, K. H., Kwon, H. J., Lee, D. H., Park, J. S., Choi, J., et al. (2015). Simultaneous Pi2 observations by the Van Allen Probes inside and outside the plasmasphere. *Journal of Geophysical Research: Space Physics*, *120*, 4567–4575. https://doi.org/10.1002/2015ja021095

Han, D. S., Iyemori, T., Gao, Y.-F., Sano, Y., Yang, F., Li, W., & Nosê, M. (2003). Local time dependence of the frequency of Pi2 waves simultaneously observed at 5 low-latitude stations. *Earth, Planets and Space*, *55*, 601.

Keiling, A., & Takahashi, K. (2011). Review of Pi2 models. *Space Science Reviews*, *161*(14), 63148. https://doi.org/10.1007/s11214-011-9818-4

Kim, K.-H., Kwon, H.-J., Lee, D.-H., Jin, H., Takahashi, K., Angelopoulos, V., et al. (2010). A comparison of THEMIS Pi2 observations near the dawn and dusk sectors in the inner magnetosphere. *Journal of Geophysical Research*, *115*, A12226. https://doi.org/10.1029/2010JA016010

Kim, K.-H., Park, J.-H., Lee, D.-H., Lysak, R., Kwon, H.-J., & Hwang, J. (2019). Magnetic field oscillations observed by Swarm satellites in the nightside upper ionosphere during low-latitude Pi2 pulsations. *Journal of Geophysical Research: Space Physics*, *124*, 6596–6612. https://doi.org/10.1029/2019JA026608

Kim, K.-H., & Takahashi, K. (1999). Statistical analysis of compressional Pc3-4 pulsations observed by AMPTE CCE at $L = 2$–3 in the dayside magnetosphere. *Journal of Geophysical Research*, *104*, 4539–4558. https://doi.org/10.1029/1998JA900131

Kwon, H.-J., Kim, K.-H., Jee, G., Park, J.-S., Jin, H., & Nishimura, Y. (2015). Plasmapause location under quiet geomagnetic conditions ($Kp \leq 1$): THEMIS observations. *Geophysical Research Letters*, *42*, 7303–7310. https://doi.org/10.1002/2015GL066090

Kwon, H.-J., Kim, K.-H., Jun, C. W., Takahashi, K., Lee, D.-H., Lee, E., et al. (2013). Low-latitude Pi2 pulsations during intervals of quiet geomagnetic conditions ($Kp \leq 1$). *Journal of Geophysical Research: Space Physics*, *118*, 6145–6153. https://doi.org/10.1002/jgra.50582

Kwon, H.-J., Kim, K.-H., Lee, D.-H., Takahashi, K., Angelopoulos, V., Lee, E., et al. (2012). Local time-dependent Pi2 frequencies confirmed by simultaneous observations from THEMIS probes in the inner magnetosphere and at low-latitude ground stations. *Journal of Geophysical Research*, *117*, A01206. https://doi.org/10.1029/2011JA016815

Lee, D.-H. (1996). Dynamics of MHD wave propagation in the low-latitude magnetosphere. *Journal of Geophysical Research*, *101*, 15,371–15,386. https://doi.org/10.1029/96JA00608

Lee, D.-H., & Lysak, R. L. (1999). MHD waves in a three-dimensional dipolar magnetic field: A search for Pi2 pulsations. *Journal of Geophysical Research*, *104*(A12), 28,691–28,699. https://doi.org/10.1029/1999ja900377

Lin, C. A., Lee, L. C., & Sun, Y. J. (1991). Observations of Pi 2 pulsations at a very low latitude ($L = 1.06$) station and magnetospheric cavity resonances. *Journal of Geophysical Research*, *96*, 21,105–21,114.

Lysak, R. L., Song, Y., Sciffer, M. D., & Waters, C. L. (2015). Propagation of Pi2 pulsations in a dipole model of the magnetosphere. *Journal of Geophysical Research: Space Physics*, *120*, 355–367. https://doi.org/10.1002/2014JA020625

Ohtani, S.-I., & Anderson, B. J. (1995). Statistical analysis of Pi 2 pulsations observed by the AMPTE CCE spacecraft in the inner magnetosphere. *Journal of Geophysical Research*, *100*(A11), 21,929–21,941. https://doi.org/10.1029/95ja01849

Olsen, N., Friis-Christensen, E., Floberghagen, R., Alken, P., Beggan, C. D., Chulliat, A., et al. (2013). The Swarm Satellite Constellation Application and Research Facility (SCARF). *Earth Planets Space*, *65*, 1189–1200.

Olson, J. V. (1999). Pi2 pulsations and substorm onsets: A review. *Journal of Geophysical Research*, *104*(17), 499.

Olson, J. V., & Rostoker, G. (1975). Pi 2 pulsations and the auroral electrojet. *Planetary and Space Science*, *23*(8), 1129–1139. https://doi.org/10.1016/0032-0633(75)90163-4

Saito, T. (1969). Geomagnetic pulsations. *Space Science Reviews*, *10*, 319.

Shinohara, M., Yumoto, K., Hosen, N., Yoshikawa, A., Tachihara, H., Saka, O., & Schuch, N. J. (1998). Wave characteristics of geomagnetic pulsations across the dip equator. *Journal of Geophysical Research*, *103*(A6), 11,745–11,754. https://doi.org/10.1029/97JA03067

Stuart, W. F. (1974). A mechanism of selective enhancement of Pi2's by the plasmasphere. *Journal of Atmospheric and Solar-Terrestrial Physics*, *36*, 851–859.

Sutcliffe, P. R., & Lühr, H. (2003). A comparison of Pi2 pulsations observed by CHAMP in low Earth orbit and on the ground at low latitudes. *Geophysical Research Letters*, *30*(21), 2015. https://doi.org/10.1029/2003GL018270

Sutcliffe, P. R., & Yumoto, K. (1989). Dayside Pi 2 pulsations at low latitudes. *Geophysical Research Letters*, *16*(8), 887–890. https://doi.org/10.1029/GL016i008p00887

Takahashi, K., Hartinger, M. D., Vellante, M., Heiling, B., Lysak, R. L., Lee, D.-H., & Smith, C. W. (2018). Roles of flow braking, plasmaspheric virtual resonances, and ionospheric currents in producing ground Pi2 pulsations. *Journal of Geophysical Research: Space Physics*, *123*, 9187–9203. https://doi.org/10.1029/2018JA025664

Takahashi, K., Lee, D.-H., Nosé, M., Anderson, R. R., & Hughes, W. J. (2003). CRRES electric field study of the radial mode structure of Pi2 pulsations. *Journal of Geophysical Research*, *108*(A5), 1210. https://doi.org/10.1029/2002JA009761

Takahashi, K., & Liou, K. (2004). Longitudinal structure of low-latitude Pi2 pulsations and its dependence on aurora. *Journal of Geophysical Research*, *109*, A12206. https://doi.org/10.1029/2004JA010580

Takahashi, K., Lysak, R., Vellante, M., Kletzing, C. A., Hartinger, M. D., & Smith, C. W. (2018). Observation and numerical simulation of cavity mode oscillations excited by an interplanetary shock. *Journal of Geophysical Research: Space Physics*, *123*, 1969–1988. https://doi.org/10.1002/2017JA024639

Takahashi, K., Ohtani, S.-I., Hughes, W. J., & Anderson, R. R. (2001). CRRES observation of Pi2 pulsations: Wave mode inside and outside the plasmasphere. *Journal of Geophysical Research*, *106*(A8), 15,567–15,581. https://doi.org/10.1029/2001ja000017

Takahashi, K., & Yumoto, K. (1999). Upper Atmosphere Research Satellite observation of a Pi2 pulsation. *Journal of Geophysical Research*, *104*, 25,035–25,045.

Teramoto, M., Takahashi, K., Nosé, M., Lee, D.-H., & Sutcliffe, P. R. (2011). Pi2 pulsations in the inner magnetosphere simultaneously observed by the Active Magnetospheric Particle Tracer Explorers/Charge Composition Explorer and Dynamics Explorer 1 satellites. *Journal of Geophysical Research*, *116*, A07225. https://doi.org/10.1029/2010JA016199

Thomas, N., Shiokawa, K., & Vichare, G. (2019). Comprehensive study of low-latitude Pi2 pulsations using observations from multisatellite Swarm mission and global network of ground observatories. *Journal of Geophysical Research: Space Physics*, *124*, 1966–1991. https://doi.org/10.1029/2018JA026094

Yeoman, T. K., & Orr, D. (1989). Phase and spectral power of mid-latitude Pi2 pulsations: Evidence for a plasmaspheric cavity resonance. *Planetary and Space Science*, *37*(11), 1367–1383. https://doi.org/10.1016/0032-0633(89)90107-4